

# Improvements of uniformity and stoichiometry for zone-leveling Czochralski growth of MgO-doped LiNbO<sub>3</sub> crystals

C.B. Tsai<sup>a</sup>, W.T. Hsu<sup>a</sup>, M.D. Shih<sup>a</sup>, C.Y. Tai<sup>a</sup>, C.K. Hsieh<sup>b</sup>,  
W.C. Hsu<sup>b</sup>, R.T. Hsu<sup>c</sup>, C.W. Lan<sup>a,\*</sup>

<sup>a</sup> Department of Chemical Engineering, National Taiwan University, Taipei 10617, Taiwan, ROC

<sup>b</sup> Sino-American Silicon Product Inc., Hsinchu, Taiwan

<sup>c</sup> Opto-Electronics & Systems Laboratories, Industrial Technology Research Institute, Hsinchu, Taiwan

Received 15 July 2005; received in revised form 14 November 2005; accepted 28 November 2005

## Abstract

The zone-leveling Czochralski (ZLCz) technique is a continuous feeding process and can be used for the growth of near-stoichiometric lithium niobate (SLN) single crystals. However, the finite crucible length can cause the variation of the zone length and thus the composition and stoichiometry, especially in the growth of a large diameter crystal. To solve the problems, several approaches were proposed for the growth of 4 cm-diameter 1 mol% MgO-doped SLN. The modification of the hot zone to minimize the zone variation was found useful for the uniformity, but the stoichiometry was inadequate even with the zone composition up to 60 mol% Li<sub>2</sub>O. A Li-excess feed was further used and a good Li/Nb ratio was obtained. Adding K<sub>2</sub>O (16 mol%) into the solution zone was useful as well, but it was inferior to using the Li-excess feed. In addition, a much lower growth rate was needed for getting an inclusion-free crystal.

© 2005 Elsevier B.V. All rights reserved.

**Keywords:** Zone-leveling Czochralski method; Growth from solution; Stoichiometry; Single crystal growth; Lithium niobate; Nonlinear-optic materials

## 1. Introduction

Lithium niobate (LiNbO<sub>3</sub>, LN) is an important material for various optical applications, such as frequency conversion, optical switches, optical modulators, and holographic storage devices [1–3]. The commercial LN crystals for these applications are usually grown from the melt at the congruent composition, i.e., Li/Nb = 48.4/51.6 [4], the so-called CLN, by the Czochralski method. However, because of the nonstoichiometry of the crystal composition, significant intrinsic defects, such as the Nb<sub>Li</sub><sup>4+</sup> anti-site defects, are generated and the crystal properties required for applications are much deteriorated. For example, these defects could lower the optical damage threshold and nonlinear efficiency, while increasing the coercive field during poling [5]. Using MgO or ZnO doping is an effective way to improve the properties [6,7]. However, the most effective way is to grow the crystal having a near-stoichiometry composition, i.e., SLN [5].

To grow an SLN crystal from a Li-rich solution, a continuous process is needed to avoid segregation. By using the double-crucible Czochralski method (DCCz) with an automatic powder supply system, Kitamura and co-workers [8,9] have reported that the SLN single crystals can be successfully pulled from a Li-rich solution (58–60 mol% Li<sub>2</sub>O). Kan et al. [10] also used the DCCz method to grow SLN crystals but with solution feeding, which was done by lifting the outer crucible during crystal growth. However, this process was not successful due to the mixing of the solution between the inner and outer crucibles. Recently, Tsai et al. [11] developed a novel process, the so-called zone-leveling Czochralski method (ZLCz), for the growth of SLN crystals. In this process, the SLN single crystal was pulled from a Li-rich solution (60 mol% Li<sub>2</sub>O), while a stoichiometric solid was fed from below in a slender crucible. Several 1 mol% MgO-doped SLN crystals (2 cm in diameter) having good diameter control and composition uniformity were grown. Because ZLCz could be easily implemented in a traditional Cz puller, its potential for industrial applications is believed to be greater than DCCz, which requires an automatic feeding system. Nevertheless, the feasibility of ZLCz for growing a large-diameter crystal has not yet been examined.

\* Corresponding author. Tel.: +886 2 2363 3917; fax: +886 2 2363 3917.  
E-mail address: cwlan@ntu.edu.tw (C.W. Lan).

Another way to grow the SLN crystal is the top-seeded solution growth method (TSSG) by using a  $K_2O$ -added flux solution [12,13]. The growth temperature being about  $1050^\circ\text{C}$  [14] was much lower than that in a Li-rich solution ( $\sim 1160^\circ\text{C}$ ). The stoichiometry of the pulled crystal was improved by increasing the  $K_2O$  concentration in the flux [15]. In a wide range of the  $K_2O$  content being about 0.16–0.195  $K_2O/LN$  flux composition in the LN melt, the grown crystal was found to be homogeneous at a near-stoichiometric composition. The maximum Li content was up to 49.99 mol% in the grown crystal for undoped SLN [16]. For the growth of MgO-doped SLN, 11 mol% of the  $K_2O$  flux was used in the melt [17–19]. The Li/Nb ratio in the grown crystals was close to the theoretical composition, i.e.,  $(Li + 2Mg)/Nb \sim 1$ , assuming Mg ions do not occupy Nb sites [17,18]. Although the  $K_2O$ -flux TSSG method seems to be a good way to grow SLN crystals, the growth rate for getting an inclusion-free crystal is very slow being less than about 0.2 mm/h [20]. This is a great obstacle for industrial applications.

In the present work, the ZLCz technique was used to grow 4 cm-diameter 1 mol% MgO-doped SLN crystals. To reduce the cost, the crucible length was made only slightly larger than its diameter, and the solid feed was short. According to our previous results for the growth of 2 cm-diameter SLN in a slender crucible [11], we noticed that the composition of the grown crystals was slightly changed due to the volume change of the solution zone. Such a volume change was mainly caused by the reduction of the radiation heat loss due to the lifting of the outer crucible; the surface area for radiation was reduced. For the growth of 4 cm-diameter SLN in the fat crucible, this thermal effect was manifest. In fact, this could be the problem of using ZLCz for the growth of large-diameter crystals in commercial applications. Therefore, in this study, several approaches were proposed to resolve this problem. In addition to the modification of the hot zone, the compositions of the solution zone and the solid feed were adjusted to improve the homogeneity and the stoichiometry of the grown crystal. In the next section, the experimental procedures are described. Section 3 is devoted to the results and discussions followed by short conclusions in Section 4.

## 2. Experimental

Raw powder of  $Nb_2O_5$  (99.995% purity, Taki Chemical Co.),  $Li_2CO_3$  (99.995% purity, Honjo Chemical Co.),  $K_2CO_3$  (99.995% purity, Sigma–Aldrich Inc.) and MgO (99.9% purity, Sigma–Aldrich Inc.) were used. After mixing the raw powder at appropriate proportions in a ball mill for 24 h, the mixed materials were calcined and sintered at  $1000^\circ\text{C}$  for 24 h. For the  $K_2CO_3$  added powders, the reaction temperature was reduced to  $800^\circ\text{C}$ .

A schematic sketch of the ZLCz growth of a 4 cm-diameter MgO-doped SLN crystal is shown in Fig. 1a, where the short double-coil set was connected to a 50 kW RF generator. The hot-zone design was found important to the growth, including the control of the zone size and thermal gradients. The outer and inner crucibles were made of platinum. The outer crucible length was 13.5 cm, inner diameter 7.9 cm, and the wall thick-

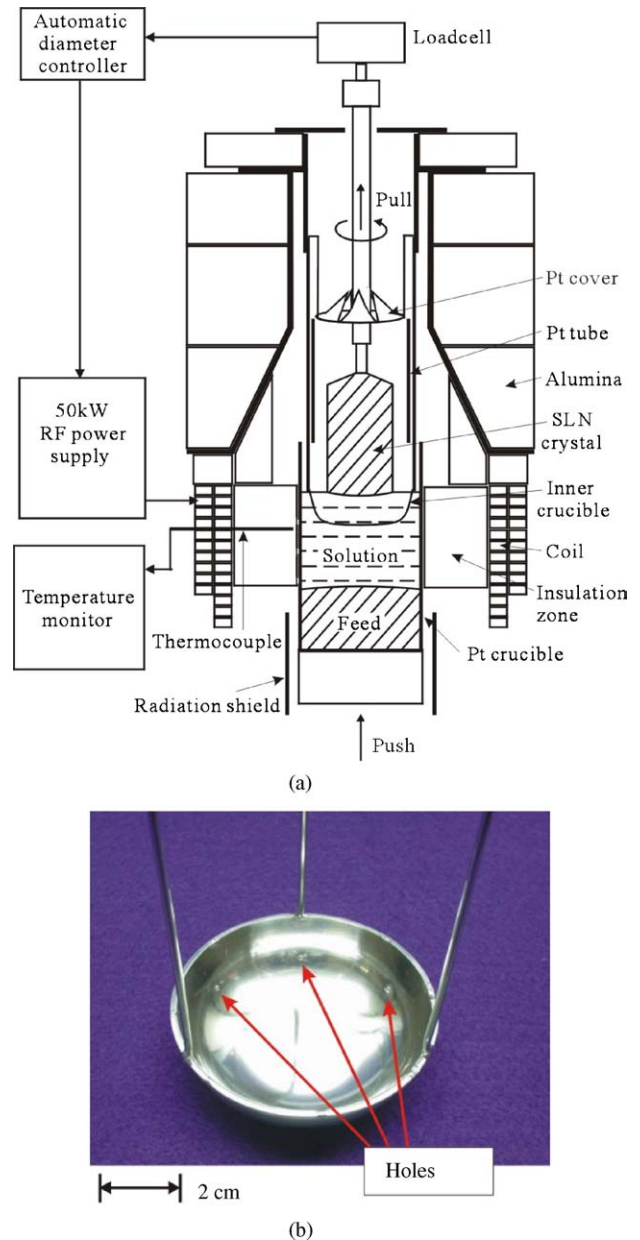


Fig. 1. (a) Schematic diagram of the zone-leveling Czochralski method; (b) platinum inner crucible with six holes (0.5 mm in diameter) at the edge of the bottom.

ness 1.5 mm. And the inner crucible had an inner diameter of 6.7 cm, height of 2 cm, and the wall thickness of 0.5 mm, as shown in Fig. 1b. The bowl shape of the inner crucible was to reduce the cost for platinum. To enforce the structure of the inner crucible, a thick ring made of a Pt/Rh alloy was used. It turned out that Rh could contaminate the melt and introduced brown color into the grown crystal, but its effect on the optical properties was not observed. The purpose of the inner crucible is to avoid the incorporation of gas bubbles generated during the melting of the solid feed [11,21].

Before crystal growth, the dense solid feed with a uniform composition was needed, and it was prepared in the outer crucible by directional solidification using a fast speed (5 cm/h). Then, the solution material was placed upon the solid feed. After

the solution zone was melted, the inner crucible was gradually immersed to a proper position by lifting the outer crucible. As the system was stabilized, a *c*-axis seed was dipped into the solution to start the growth. An automatic diameter control (ADC) system developed in our research group was used to control the crystal diameter. During growth, the outer crucible was moved upward, and the lifting speed was varied according to the mass pulling rate of the crystal. The seed was rotated at 6–10 rpm and the pulling rate was 0.2–0.6 mm/h.

To finish the growth, the crystal was detached from the solution surface. Then, the outer crucible was lowered slowly to separate the inner crucible from the solution zone. The grown crystal was cooled in the furnace to room temperature in 24 h, and was then annealed in a box furnace at 1000 °C for 24 h to release thermal stress. The grown crystal surface was often covered by a thin layer of white  $\text{Li}_3\text{NbO}_4$ , and it could be removed easily by an HF aqueous. After removing the deposition, the crystal was transparent but yellowish in color due to the Rh contamination from the ring on the inner crucible. The crystal was then oriented by X-ray again, and sliced into several wafers perpendicular to the growth direction by using a precision annular ID saw (Model APD1, Logitech Co.). The wafers were lapped and polished to 1 mm in thickness by a precision lapping and polishing machine (Model PM5, Logitech Co.) for optical measurements.

The absorbance of the wafers was measured by a spectrometer (Model V-570, Jasco Co.), and the absorption coefficient could be obtained by dividing the absorbance by the wafer thickness. The absorption edge was determined at  $20 \text{ cm}^{-1}$  of the absorption coefficient. Because the resolution of the wavelength was 0.1 nm, the absorption edge could be measured accurately. The ordinary ( $n_o$ ) and extraordinary ( $n_e$ ) indices were measured by a prism coupler (Model 2010, Metricon Co.) using a He–Ne laser (632.8 nm) as the light source. In addition, the powder samples taken from the wafers were used for Curie temperature measurement using a differential scanning calorimeter (Model HT-DSC 404, Netzsch Instrument Inc.). For composition measurements (Li, Nb and Mg), ICP-AES (Model ICAP 9000, Thermo Jarrell-Ash Co.) was used, where the powder samples were fluxed melted and then diluted by DI water according to the procedure mentioned in [22].

### 3. Results and discussion

Table 1 summarizes the growth conditions of the crystals in this work. Crystals 1 and 2 were grown from the original and modified hot zones, respectively. Crystal 3 was grown by using a Li-excess solid feed. Crystal 4 was grown from the  $\text{K}_2\text{O}$ -added

Table 1  
Growth conditions of grown crystals

	Radiation shield	$\text{K}_2\text{O}$ -flux	Li-excess feed
Crystal 1	×	×	×
Crystal 2	✓	×	×
Crystal 3	✓	×	✓
Crystal 4	✓	✓	×

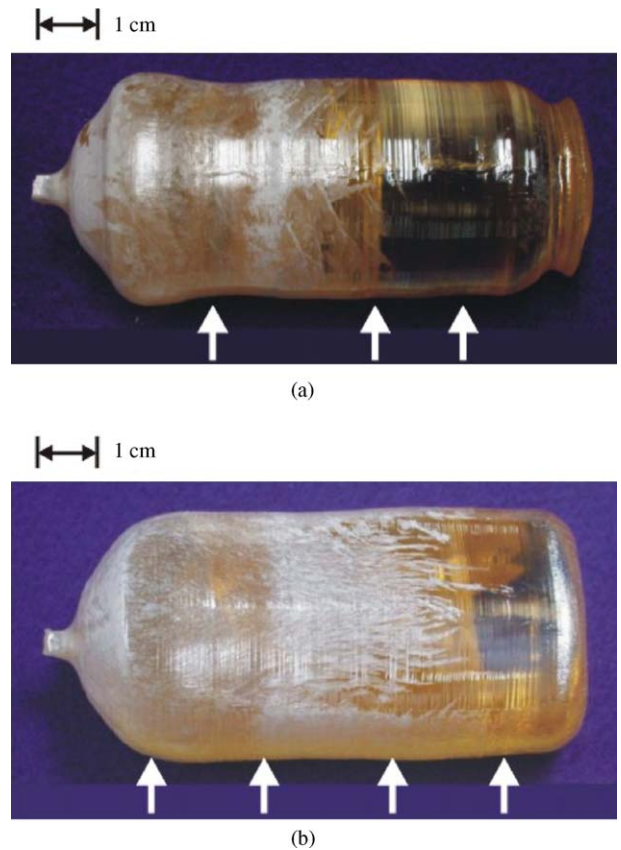


Fig. 2. As-grown 1 mol% MgO-doped SLN crystals: (a) crystal 1: using the original hot zone; (b) crystal 2: with the lower radiation shield; 60 mol%  $\text{Li}_2\text{O}$  solution zone was used and the growth rate was 0.6 mm/h. The white arrows show the sampling positions for measurements.

solution zone. Their growth and characterization results will be discussed shortly.

Fig. 2 shows the as-grown crystals pulled from a Li-rich (60 mol%  $\text{Li}_2\text{O}$ ) solution at 0.6 mm/h using the SLN solid feed. The first crystal (referred as crystal 1) shown in Fig. 2a was grown without using the radiation shield (also see Fig. 1a). Some white  $\text{Li}_3\text{NbO}_4$  deposition appeared on the crystal, and it was caused by the excess Li used in the solution zone. As shown, the deposition was not uniform and disappeared in the second half of the crystal. Apparently the Li content in the solution zone for the second half of the crystal was lower. This dilution effect was because more solid feed was dissolved due to the increase of the solution zone, which was caused by the change of the thermal condition. As shown in Fig. 1a, without the radiation shield, as the feed was lifted, the radiation heat loss from the crucible surface below the insulation zone was reduced. For the whole growth period, the reduction of the radiation heat loss was more than 60%. As a result, the zone length increased significantly leading to the composition change in the solution zone and thus the crystal.

To overcome the problem, a radiation shield, as shown in Fig. 1a, was used. The shield was made of alumina with a single cylinder shape. And it was fixed to keep a constant area of the radiation heat loss below the insulation zone. In addition, the initial zone size was slightly increased, so that the lower interface

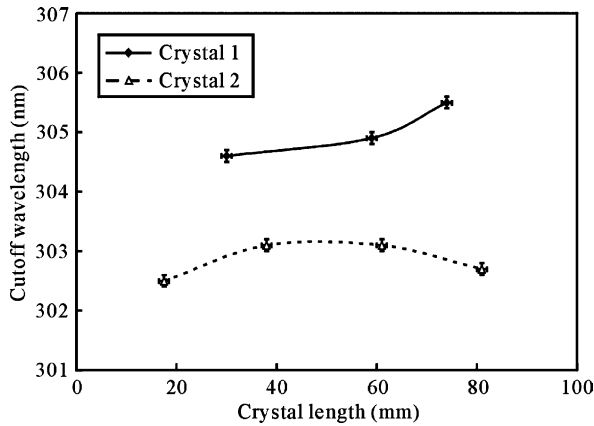


Fig. 3. Axial distributions of cutoff wavelength for crystals 1 and 2.

of the zone was closer to the edge of the insulation zone having a larger thermal gradient. Because of the larger thermal gradient for the lower interface and the constant area for the radiation heat loss, the change of the zone size during growth was significantly reduced. The grown crystal (referred as crystal 2) based on this condition is shown in Fig. 2b. As shown, the uniformity of the  $\text{Li}_3\text{NbO}_4$  on the crystal surface was significantly improved as compared to that in crystal 1.

The absorption edge, or the so-called cutoff wavelength, of crystals 1 and 2 was further measured, and summarized in Fig. 3. As expected, crystal 2 has a better uniformity. The cutoff values of crystal 1 were about 304.6–305.5 nm being slightly higher than the reported values, i.e., 304 and 300.8 nm for 0.78 and 1.98 mol% MgO-doped SLN, respectively [17], and 302.5 and 301.5 nm for 0.6 and 1.8 mol% MgO-doped SLN, respectively [23]. Nevertheless, Wang et al. [24] obtained the cutoff value at 305 nm for a 1 mol% MgO-doped SLN crystal grown from an 11 mol%  $\text{K}_2\text{O}$ -flux solution. The absorption edge usually decreases with the increasing MgO doping and Li/Nb ratio [5,17]. Since the MgO content along the grown crystal was small due to the near unity segregation coefficient and the continuous feeding [17], the variation of the cutoff values along the crystal was likely to be the change of the Li/Nb ratio. This speculation was also consistent with the deposition of  $\text{Li}_3\text{NbO}_4$  on the crystal surface shown in Fig. 2a. According to [5], 1 nm variation of the cutoff wavelength corresponds to about 0.5% change of the Li/Nb ratio in the crystal. Therefore, in crystal 1, the Li/Nb ratio decreased along the crystal. Also, due to the high cutoff value at the beginning, the solution had been diluted by the feed even at the seeding stage.

On the other hand, the cutoff values of crystal 2 shown in Fig. 3 were much lower and more uniform than that of crystal 1. The decrease of the cutoff values corresponds to about 0.75–1% increase on the Li/Nb ratio. Nevertheless, the value being about 303 nm is still not low enough as compared with the value reported in [17]. To get a better idea of the relationship between the cutoff value and the Li/Nb ratio, we have summarized the measured data in Fig. 4 for 0.91–1.10 mol% MgO doped SLN crystals available in our laboratory; the data points (different MgO contents) reported by Niwa et al. [17] are also included for comparison. As shown, the Li/Nb ratio in

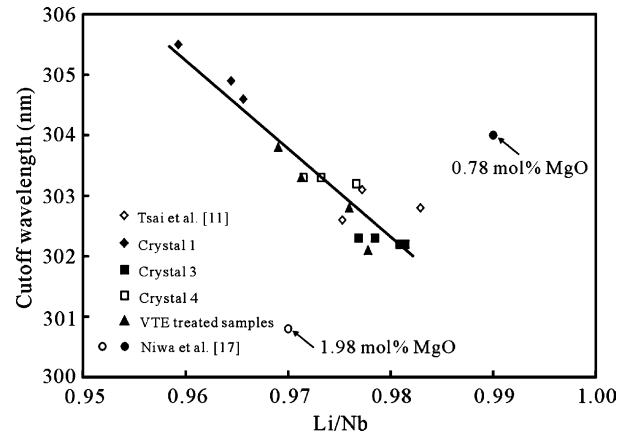


Fig. 4. Absorption edge as a function of the Li/Nb ratio in the SLN crystals with 0.91–1.10 mol% MgO doping. The vapor transport equilibrium (VTE) [5] treated samples are also included for comparison. Crystals 3 and 4 were obtained by the Li-excess solid feed and  $\text{K}_2\text{O}$ -added solution, respectively, which will be discussed shortly.

crystal 2 corresponding to the cutoff value at 303 nm is only 0.975.

To further increase the Li/Nb ratio, two approaches were considered. One was to increase the Li content in the solid feed and the other was to use  $\text{K}_2\text{O}$ -added solution zone. Fig. 5a shows the crystal (referred as crystal 3) grown from a Li-rich solution using a Li-excess ( $\text{Li}/\text{Nb} = 51/49$ ) solid feed; again the growth rate was 0.6 mm/h. As shown, the surface of crystal 3 was also covered by a thin layer of  $\text{Li}_3\text{NbO}_4$  on the shoulder of the crystal, but was much less on the body. It was presumed that  $\text{Li}_3\text{NbO}_4$  having a much higher melting point was floating upon the solution surface. Thus, the deposition on the shoulder part could have depleted  $\text{Li}_3\text{NbO}_4$  inside the inner crucible. As the crystal grew further, the excess  $\text{Li}_3\text{NbO}_4$  formed due to the excess Li from the feed was kept away by the inner crucible. As a result, the rest crystal did not have much  $\text{Li}_3\text{NbO}_4$  deposition on the surface. The crystal grown from 16 mol%  $\text{K}_2\text{O}$ -added solution is shown in Fig. 5b (referred as crystal 4). For comparison, three growth speeds being 0.2, 0.4 and 0.6 mm/h were used at different stages of the growth. As shown, the appearance of crystal 4 is quite different from the previous crystals. There was no  $\text{Li}_3\text{NbO}_4$  deposition on the crystal surface.

The absorption edge and the Curie temperature along the growth axis of crystals 3 and 4 are shown in Fig. 6. The cutoff values for both crystals were quite uniform being about 302.25 and 303.25 nm, respectively for crystals 3 and 4, having only 0.1 nm deviations. Similarly, the Curie temperatures of crystals 3 and 4 were also quite high being about 1212.4 and 1210.8 °C, respectively, and the variations are within the measurement error. These Curie temperatures are also in good agreement with the reported values, i.e., 1206 and 1213 °C for 0.78 and 1.98 mol% MgO-doped SLN, respectively [17,18]. In addition, according to O'Bryan equation [25], 4 °C increase in the Curie temperature corresponds to about 0.5% increase in the Li/Nb ratio. Therefore, the high Curie temperature with a small deviation further indicates the high Li/Nb ratio and good uniformity along the crystals. Interestingly, the crystal grown from the Li-excess

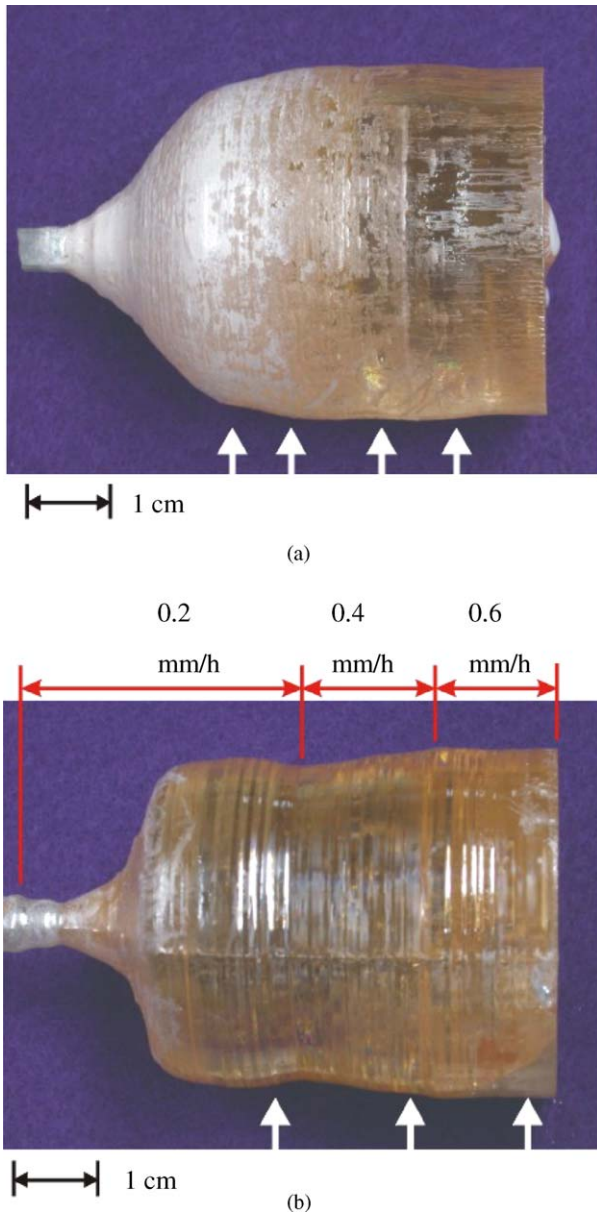


Fig. 5. As-grown 1 mol% MgO-doped SLN crystals: (a) crystal 3: using the Li-excess solid feed (growth rate was 0.6 mm/h); (b) crystal 4: using the  $K_2O$ -flux solution (growth rates were indicated). The white arrows show the sampling positions for measurements.

solid feed, i.e., crystal 3, seems to be slightly better than that grown from the  $K_2O$ -added solution.

The measured Li/Nb and Mg/Nb ratios along the crystals, as shown in Fig. 7, further confirmed the previous conclusion. The Li/Nb ratio of crystal 3 was around 0.977–0.981, and the Mg/Nb ratio was about 1.01–1.10%. For crystal 4, the Li/Nb ratio was about 0.971–0.977 and the Mg/Nb ratio was about 0.91–0.97%. Again, crystal 3 was slightly better than crystal 4 in the stoichiometry. Nevertheless, it should be pointed out that the relative measurement error in the concentration is still larger than that in the cutoff value. In fact, the deviations of Li/Nb along the crystals in Fig. 7 were within the measurement errors. Polgar and co-workers [16] have claimed that the unity stoichiometry of

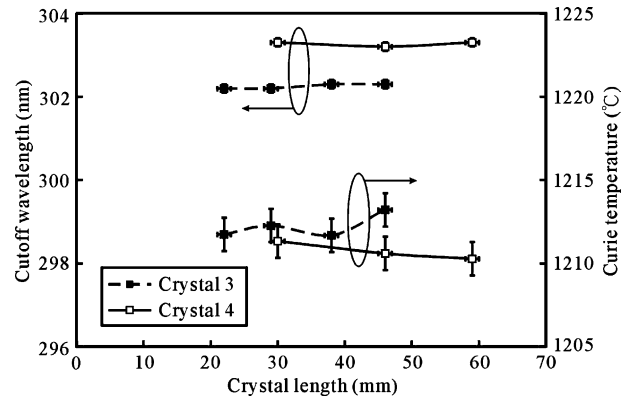


Fig. 6. Axial distributions of absorption edge and Curie temperature in crystals 3 and 4.

the undoped SLN crystal pulled from 16 mol%  $K_2O$ -flux solution could be achieved. The 1 mol% MgO-doped SLN crystal pulled from the same flux solution should be having the Li/Nb ratio to near 0.98 which was the theoretical limit estimated from the defect model [17,18]. Indeed, crystal 4 showed a Li/Nb ratio being close to 0.98, but it was not the best value as compared with crystal 3. Thus, the flux concentration reported by Polgar and co-workers [16] may be not the best condition for growing MgO-doped SLN crystals. Although the stoichiometry of crystal 4 was not as good as crystal 3, the uniformity was significantly improved as compared with crystals 1 and 2. To further confirm the uniformity and stoichiometry, refractive indices were also measured. The ordinary index  $n_o$  was about 2.2859 and the extraordinary index  $n_e$  about 2.1889 for crystal 3. For crystal 4,  $n_o$  was about 2.2859 and  $n_e$  about 2.1913. These values were also quite close to the reported ones;  $n_o = 2.2865$  and  $n_e = 2.1898$  for 1 mol% MgO-doped SLN [26];  $n_e = 2.189 \pm 0.0004$  for undoped SLN [27,28]. Nevertheless, the deviations along the crystals were within the measurement errors.

Furthermore, the radial cutoff distributions of the grown crystals were also measured. As shown in Fig. 8, the cutoff values in the radial direction were quite uniform for all crystals, even for crystal 1 that had non-trivial axial nonuniformity. The small deviations in the radial cutoff wavelengths correspond to a composition variation of less than 0.1%. The good radial uniformity could be considered a great advantage of ZLCz for SLN growth.

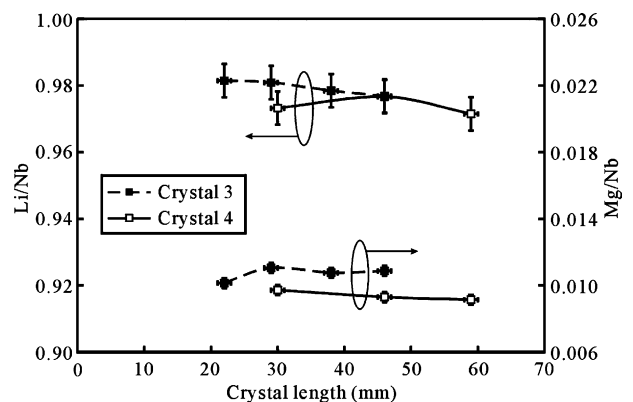


Fig. 7. Axial distributions of Li/Nb and Mg/Nb ratios in crystals 3 and 4.

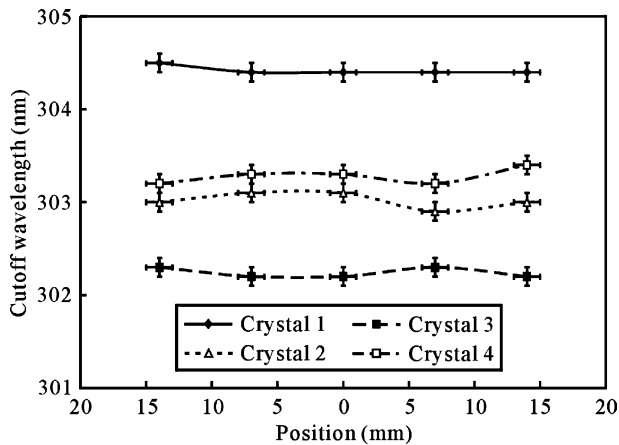


Fig. 8. Radial distributions of cutoff wavelength for grown crystals. Position 0 was the center of the wafer.

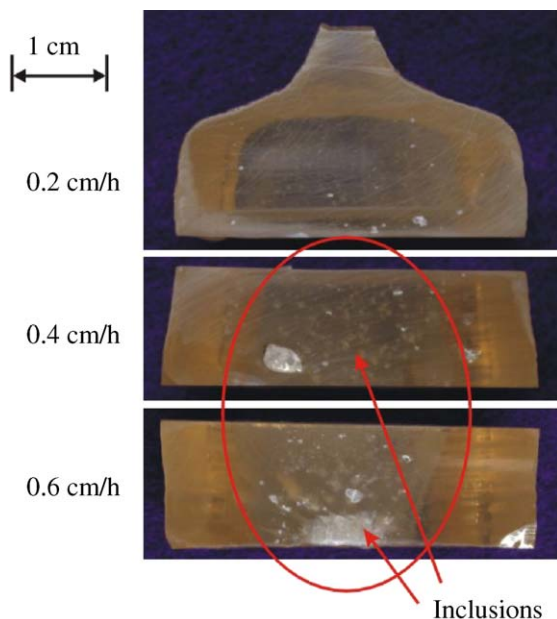


Fig. 9. Cross sections of crystal 4 at different growth rates.

Although crystal 4 showed similar properties and uniformity as crystal 3, its crystal quality was not good. The cross section of the crystal is shown in Fig. 9. As shown, significant inclusions were easily observed in crystal 4 when the growth speed was higher than 0.2 mm/h. Therefore, from the production point of view, the growth using the  $K_2O$ -added flux solution is not practical. On the other hand, by using a Li-excess solid feed and a proper hot-zone design, a crystal having a Li/Nb ratio up to 0.98, which is close to the theoretical limit, and a good composition uniformity could be easily grown by the ZLCz technique.

#### 4. Conclusions

Several methods for improving composition uniformity and stoichiometry in ZLCz SLN growth were proposed. A proper hot-zone design was found necessary especially when the feed

solid was not long. Using the lower radiation shield for keeping a constant radiation heat loss below the insulation zone and using a large thermal gradient at the melt/feed interface were found crucial to reduce the zone variation during crystal growth. Further improvement of the Li/Nb ratio to near 0.98 could be achieved by using a Li-excess SLN solid feed or a  $K_2O$ -flux solution zone. However, the pulling rate for growing an inclusion-free SLN crystal from the  $K_2O$ -flux solution was much lower than that from the Li-rich solution.

#### Acknowledgements

This work was mainly supported by the National Science Council of Taiwan and Sino-American Silicon Products Inc. Partial support from National Taiwan University and the Materials Research Laboratories and the Opto-Electronics & Systems Laboratories of the Industrial Technology Research Institute is also acknowledged.

#### References

- [1] V. Gopalan, M. Kawas, T.E. Schlesinger, M.C. Gupta, D.D. Stencil, *IEEE Photonics Technol. Lett.* 8 (1996) 1704–1706.
- [2] K. Kintaka, M. Fujimura, T. Suhara, H. Nishihara, *J. Lightwave Technol.* 14 (1996) 462–468.
- [3] J.F. Heanue, M.C. Bashaw, L. Hesselink, *Science* 265 (1994) 749–752.
- [4] P.F. Bordui, R.G. Norwood, C.D. Bird, G.D. Calvert, *J. Cryst. Growth* 113 (1991) 61–68.
- [5] Y.L. Chen, J.P. Wen, Y.F. Kong, S.L. Chen, W.L. Zhang, J.J. Xu, G.Y. Zhang, *J. Cryst. Growth* 242 (2002) 400–404.
- [6] Y.L. Chen, J. Guo, C.B. Lou, J.W. Yuan, W.L. Zhang, S.L. Chen, Z.H. Huang, G.Y. Zhang, *J. Cryst. Growth* 263 (2004) 427–430.
- [7] L.H. Peng, Y.C. Zhang, Y.C. Lin, *Appl. Phys. Lett.* 78 (1) (2001) 4–6.
- [8] K. Kitamura, J.K. Yamamoto, N. Iyi, S. Kimura, T. Hayashi, *J. Cryst. Growth* 116 (1992) 327–332.
- [9] Y. Furukawa, M. Sato, K. Kitamura, F. Nitanda, *J. Cryst. Growth* 128 (1993) 909–914.
- [10] S. Kan, M. Sakamoto, Y. Okano, K. Hoshikawa, T. Fukuda, *J. Cryst. Growth* 128 (1993) 915–919.
- [11] C.B. Tsai, Y.T. Hsia, M.D. Shih, C.Y. Tai, C.K. Hsieh, W.C. Hsu, C.W. Lan, *J. Cryst. Growth* 275 (2005) 504–511.
- [12] G.I. Malovichko, V.G. Grachev, E.P. Kokanyan, O.F. Schirmer, K. Betzler, B. Gather, F. Jermann, S. Klauer, U. Schlarb, M. Wöhlecke, *Appl. Phys. A* 56 (1993) 103–108.
- [13] K. Polgar, A. Peter, I. Foldvari, Zs. Szaller, *J. Cryst. Growth* 218 (2000) 327–333.
- [14] K. Polgar, A. Peter, L. Poppl, M. Ferriol, I. Foldvari, *J. Cryst. Growth* 237–239 (2002) 682–686.
- [15] M.D. Serrano, V. Bermudez, L. Arizmendi, E. Dieguez, *J. Cryst. Growth* 210 (2000) 670–676.
- [16] A. Grisard, E. Lallier, K. Polger, A. Peter, *Electron. Lett.* 36 (n12) (2000) 1043–1044.
- [17] K. Niwa, Y. Furukawa, S. Takekawa, K. Kitamura, *J. Cryst. Growth* 208 (2000) 493–500.
- [18] Y. Furukawa, K. Kitamura, S. Takekawa, K. Niwa, Y. Yajima, N. Iyi, I. Mnushkina, P. Guggenheim, J.M. Martin, *J. Cryst. Growth* 211 (2000) 230–236.
- [19] D. Sun, J. Xiao, L. Zhang, Y. Hang, S. Zhu, A. Wang, S. Yin, *J. Cryst. Growth* 262 (2004) 240–245.
- [20] S. Solanki, T.C. Chong, X. Xu, *J. Cryst. Growth* 250 (2003) 134–138.
- [21] C.W. Lan, H.J. Chen, C.B. Tsai, *J. Cryst. Growth* 245 (2002) 56–62.
- [22] T. Ashino, K. Takada, *Anal. Sci.* 9 (1993) 737–739.

- [23] Y. Furukawa, K. Kitamura, S. Takekawa, K. Niwa, H. Hatano, *Opt. Lett.* 23 (1998) 1892–1894.
- [24] H. Wang, Y. Hang, L. Zhang, J. Xu, M. He, S. Zhu, Y. Zhu, S. Zhou, *J. Cryst. Growth* 262 (2004) 313–316.
- [25] H.M. O'Bryan, P.K. Gallagher, C.D. Brandle, *J. Am. Ceram. Soc.* 68 (1985) 493–496.
- [26] M. Nakamura, S. Higuchi, S. Takekawa, K. Terabe, Y. Furukawa, K. Kitamura, *Jpn. J. Appl. Phys.* 41 (2002) L49–L51.
- [27] A. Yamada, H. Tamada, M. Saitoh, *J. Cryst. Growth* 132 (1993) 48–60.
- [28] D.H. Jundt, M.M. Fejer, R.L. Byer, *J. Quantum IEEE Electron. QE-26* (1990) 135–138.